Article:
Nourafkan, E, Gardy, J orcid.org/0000-0003-1806-4056, Asachi, M et al. (2 more authors) (2019) Nanoparticle Formation in Stable Microemulsions for Enhanced Oil Recovery Application. Industrial & Engineering Chemistry Research, 58 (28). pp. 12664-12677. ISSN 1520-5045

https://doi.org/10.1021/acs.iecr.9b00760

Nanoparticles formation in stable microemulsions for Enhanced Oil Recovery application

Ehsan Nourafkan[*†], Jabbar Gardy[‡], Maryam Asachi[‡], Waqar Ahmed[†], Dongsheng Wen[*‡, §]

[†]School of Mathematics and Physics, University of Lincoln, Lincoln, LN6 7TS, UK.

[‡]School of Chemical and Process Engineering, University of Leeds, Leeds, LS2 9JT, UK.

[§] School of Aeronautic Science and Engineering, Beihang University, Beijing, 100191, China.

Abstract

Magnetic iron oxide and titanium dioxide nanoparticles (NPs) have been synthesised inside stable oil-in-water microemulsions in harsh environment of high temperature-high salinity (HT-HS). Screening of anionic-nonionic mixture of commercial surfactants was carried out to identify the appropriate compositions for production of stable microemulsions in harsh environment. The effect of salinity and NPs formation on interfacial tension and rheological properties of microemulsions have been evaluated and the results were compared with those obtained in other studies. It was found that oil-in-water microemulsions exhibited a non-Newtonian shear thinning behaviour while the surfactant solutions show the Newtonian behaviour. The shear-thinning characteristic of microemulsions was improved and the interfacial tension between microemulsions and oil phase was increased after generation of NPs. A set of flooding experiments were accomplished using a microfluidic device to assess the efficiency of enhanced oil recovery at the pore scale in absence and presence of NPs. The flooding tests confirmed the improvement of oil recovery efficiency after the formation of NPs inside the microemulsions. The oil displacement of API flooding was equal to 69.8% and the maximum oil displacement of 76.9% was observed after the injection of microemulsion containing iron oxide NPs.

Keywords: Microemulsion stability, Nanoparticles, Synergistic effect, Harsh environment, Rheological behaviour, Interfacial tension.

1. Introduction

Microemulsions (MEs) are thermodynamically stable colloidal dispersions which are generated by mixing of oil and aqueous phase in presence of stabilizers including surfactant and/or co-surfactant. The droplets size of disperse phase are less than 100 nm (wavelength of visible light) and this is why the microemulsion are transparent, unlike macroemulsions.[1,2] Comparing to surfactant (micelles) flooding, MEs have distinct advantages including lower interfacial tension (IFT) and higher viscosity, which makes them more efficient for enhanced oil recovery (EOR) application.[3,4] For example, Exxon company successfully applied the MEs flooding in pilot scale for oil recovery operation in Loudon Field, Illinois, USA.[5]

Typically, a reservoir's temperature is in the range of 10-120 ºC and the amount of brine salinity is between 0.3 and 21 wt%.[6] Most of common stabilizers (e.g. sodium dodecyl sulphate) could not chemically resist over harsh environment in depth of oil reservoir. As a result, those emulsions which were synthesized using conventional stabilizers would be degraded gradually in harsh environment such as HT-HS. The majority of research on chemical EOR using surfactant flooding have applied conventional stabilizers for synthesis and stabilization of emulsions under normal conditions (e.g. ambient temperature). However, the harsh reservoir condition could easily deform the stability and rheological behaviour of such MEs, leading to poor mobility control. [7]

Incorporation of NPs in the structure of emulsion could reinforce their properties such as rheological behaviour and stability. [8-10] Several researches reported that NPs could increase the conformance control[11], improve the emulsion's stability in harsh condition [12-14] or reduce the surfactant consumption during the core-flooding process.[15-17] However, a careful literature review showed that this area is still in its infancy with many problems unsolved, ranging from the manufacturing of stable NPs-MEs systems, understanding their rheological properties of MEs, and mechanisms of NPs-MEs interactions. Highly related to this work, it showed that:

-All MEs are still suffering stability issues under reservoir conditions. It has reported by Barnes et al.[18] that the internal olefin sulfonate (IOS) stabilizers category could resist over de-stability at high temperature condition even up to 150 °C. On the other hand, non-ionic alkoxylated surfactants have good stability at high concentration mono- and di-valent salts.19 The synergistic effect between aforementioned stabilizers combination for synthesis of long-term stable MEs-NPs at HT-HS condition has not been carefully studied.

-All studied have utilized two-steps method for preparation of NPs-emulsion by dispersing commercial dry nanopowders into the emulsions. There is still no one-step method reported, where NPs are generated inside the required fluid. It is more favourable due to their advantages such as reducing the cost of manufacturing and mixing of dry nanopowders.[20] Moreover, direct synthesis of NPs inside the emulsions could promote the NP's stability since the emulsion environment act as mother liquid for chemical reaction between precursors. Following by reaction the primary nuclei is formed and growth of nuclei simultaneously occur. Finally, the NPs would appear inside the emulsion that have more compatible surface chemistry with mother liquid comparing to commercial dry nanopowders.

This study aims to fill the aforementioned gaps by investigating the effect of in-situ formation of NPs on the rheological behaviour of MEs. The general framework of current research is as follows:

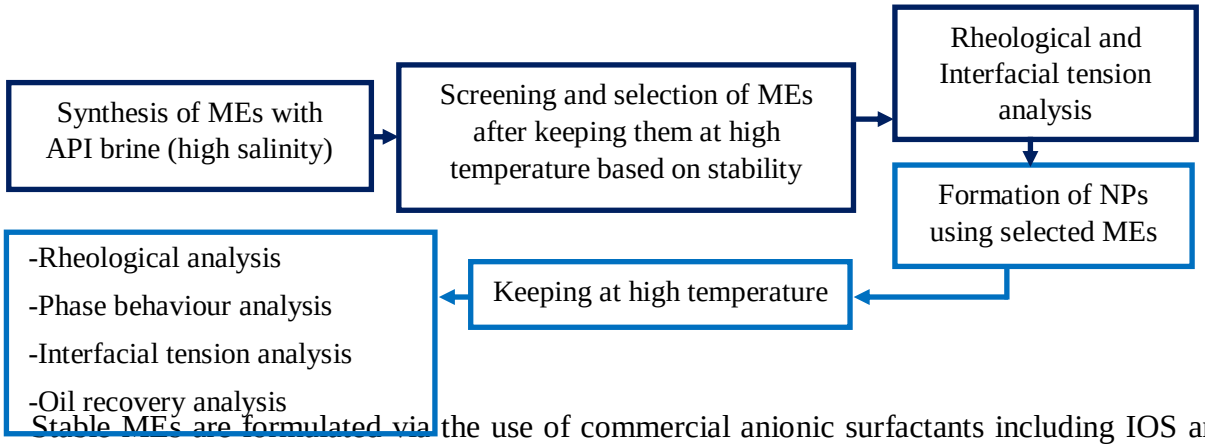

Stable MEs are formulated via the use of commercial anionic surfactants including IOS and alcohol alkoxy sulfate (AAS) with non-ionic ones including ethoxylate alcohol and alkoxylated di-nonylphenol at HT-HS. IOS are twin-tailed surfactants which have appropriate solubilization as well as resistance over depredation at high temperature. After screening of high stable MEs in API brine at 70 °C (HS-HT) the iron oxide (IO) and titanium dioxide (TiO_2) NPs were synthesized inside the selected MEs. The composition of API brine will be explained in part 2.2. Finally, the NPs-ME influence on crude oil displacement was observed visually using microfluidic flooding test and evaluated by image processing in compare to MEs alone and API brine.

2. Experimental work

2.1. Materials and characterization

Table 1 and Figure 1 show the commercial surfactants information applied in this study.

Internal olefin sulfonate

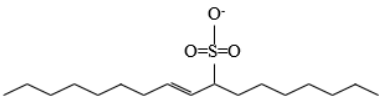

Alcohol alkoxy sulfate

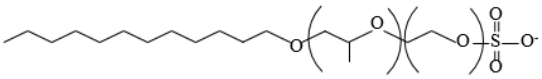

Ethoxylated alcohol

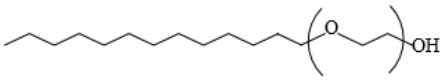

Alkoxylated di-nonylphenol

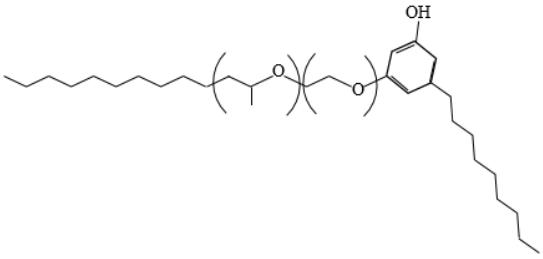

Figure 1. The chemical structure of commercial surfactants

Table 1. The commercial surfactants used in this study.

Commercial name	O332	O342	J071	XOF 320
Type	IOS[a]	IOS	AAS[b]	Alkoxylated di-nonylphenol
Number of carbon atom in tail structure	15-18	19-23	12-13	10
Number of ethoxylated group	0	0	7	Unknown
Manufacturer	Shell Co.	Shell Co.	Shell Co.	Huntsman Co.
Commercial name	N23-7	Neodol 91-8 (ND 91-8)	Neodol 25-12 (ND 25-12)	
Type	Ethoxylated alcohol	Ethoxylated alcohol	Ethoxylated alcohol	
Number of carbon atom in tail structure	12-13	9-11	12-15	
Number of ethoxylated group	7	8	12	

Manufacturer	Mistral chemical Co.	Shell Co.	Shell Co.

[a] Internal olefin sulfonate, [b]Alcohol alkoxy sulfate

Analytical grade materials including n-hexane, n-octane, 2-butanol, sodium hydroxide, calcium chloride, magnesium chloride, sodium chloride and sodium hydroxide were purchased from Sigma-Aldrich. The iron (III) 2-ethylhexanoate and titanium (IV) 2-ethylhexanoate were provided from Alfa Aesar Ltd and crude oil was purchased from Texas raw crude oil Company.

Rheological Analysis. Physica Anton Paar rheometer (Cone plate CP75-1, model MCR 301) was used for measurement of rheological properties of MEs and NPs-MEs including viscosity and viscoelastic modulus (G′, G″). The shear rate (γ) was varied between 10 and 1000 s^{-1} and frequencies of 1 -100 rad/s were considered for viscosity and dynamic viscoelastic evolution at room temperature, respectively.**Interfacial Tension (IFT).**

The pendant drop tests were performed using CAM 2008 Goniometer to investigate the interfacial tension on samples at room temperature. A set of standard stainless steel balls (0.0625, 0.0937 and 0.1564 inch) were used to perform calibration test of Goniometer system. The calibration standard balls covered the sizes range of pendant droplets.

Hydrodynamic Size and TEM analysis.

Hydrodynamic size of nanodroplets were measured using Malvern Zetasizer and the morphology and size distribution of NPs were evaluated using Transmission electron microscope (FEI Tecnai TF20 TEM, LEMAS facilities). Sample preparation is a necessary prerequisite for TEM analysis. In order to prepare the TEM samples, the original MEs were sonicated after twice dilution with deionized water. Dilution with water reduced the effect of surfactants layer on TEM images. Holey carbon support film on copper grids was used to prepare TEM samples. A few drops of the diluted suspension were placed over TEM grid and then left it to dry at room temperature. As water and n-hexane are volatile, the images included nanoparticles with a fraction of stabilizers.

Phase Behaviour. Glass pipette procedure was carried out for phase behaviour evaluation which will be discussed in part 3.5.

Microfluidic Chip. Recent developments in optical microscopy provide techniques for direct visualization of oil recovery in microchips as model porous media.[24,25] Figure 2a shows the microfluid flooding experimental rig and utilized microchip. The cuvette slide chip (cyclo-

olefin copolymer, ThinXXs Ltd, Germany) consisting of five rectangular and spherical chambers was used as sample pore during flooding tests (Figure 2b). Three different syringes (500 µl, Hamilton) were used for injection of crude oil, API brine and ME which were connected to the microchip through PTFE tubing (outside diameter: 1/16" (1.6mm)-inside diameter: 0.8mm). The displacement pattern was monitored through direct visualization by taking images with an Olympus SZX16 microscope. A light is set just under micromodel to help taking high resolution images. The images were taken by a digital camera during fluiding test through micromodel. FlyCapture 2.5.3.4 software was used to program digital camera to take scheduled shots up to end of flooding test. The fluid flooding was performed with a syringe pump (Nexus 6000, Chemyx Ltd.) at ambient temperature according to the following procedure:

-The crude oil was injected to fill both the oil-wet microchannels and then chambers between the microchannels. The outlet crude oil was collected in a waste storage vessel at atmosphere pressure.

-The API brine as well as microemulsion (before and after NPs generation), were then injected into the microchannel. A 3D valve was used to prevent the formation of air bubble during the change of syringe (injection fluid). In order to evaluate the oil recovery and compare the oil displacement efficiency, the crude oil fraction of each image was estimated using image processing (Figure 2c).[26,27] The rate of fluid injection inside the microchannel was considered

17 µl/hour which is equivalent to 1 m/day in real industrial condition.

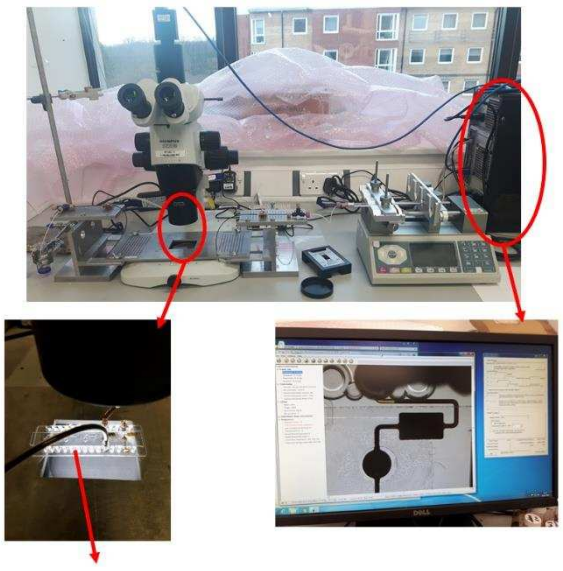

(a)

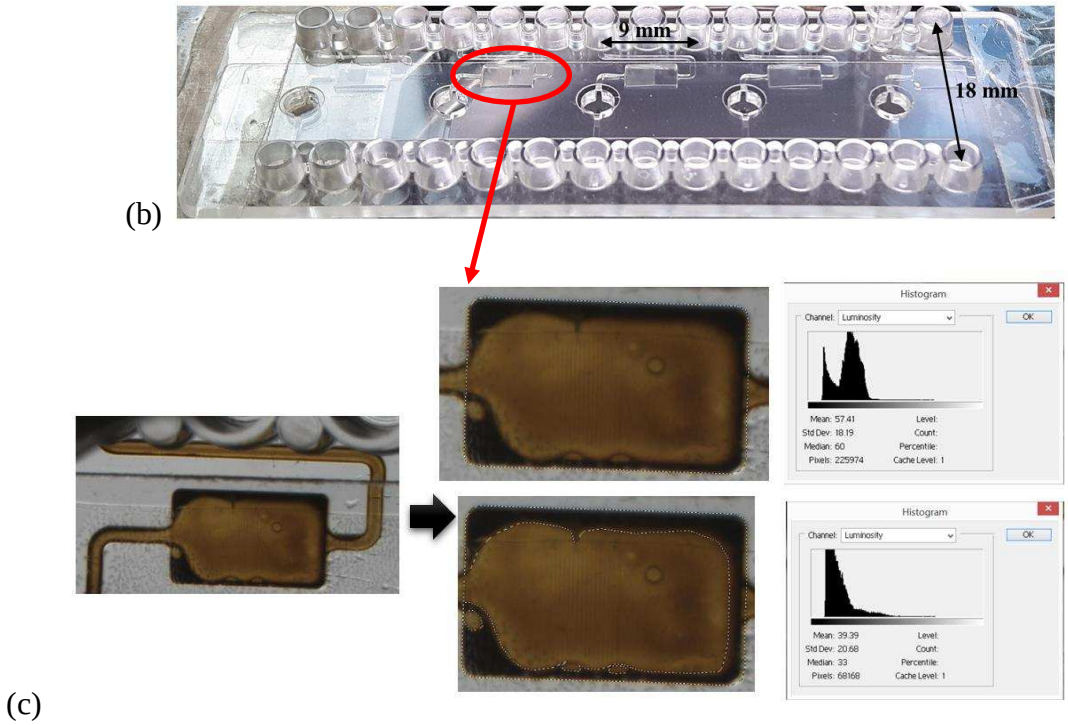

Figure 2. (a) Microfluidic flooding rig set up, (b) Cuvette slide chip, and (c) Image processing to estimate of crude oil displacement after flooding tests.

2.2. Microemulsion screening

The API brine was prepared by solving sodium chloride (8 wt.%), CaCl2 and MgCl2 (both 2 wt.%) in dionized water. A set of oil-in-water (O/W) MEs were synthesized at API brine andkept at high temperature (70 °C) for 48 hours to screen the stable samples in HT-HS. The composition of MEs was fixed as 97 wt.% API brine, 0.8 wt.% n-hexane (oil phase), 0.75 wt.% n-butanol (co-solvent) and 1.45 wt.% surfactant blends (equal amount of anionic and non-ionic types). The mixtures were mixed for 4 h to complete reaction and reach the equilibrium, then, each solution was divided into two parts. One part of samples was retained at room temperature while the other sample was kept immobile at 70 ºC inside an oven for 48 hours. Screening of surfactants blend was performed based on observing the instability of samples by naked eyes. Stable MEs were selected for further analysis and NPs formation in next parts of experiments.

2.3. Synthesis of nanoparticles inside microemulsion

The procedure of NPs formation inside the O/W MEs was described in our previous study in detail.[12] Herein, iron (III) and titanium (IV) 2-ethylhexanoate were used as precursor for formation of IO and TiO_2 NPs, respectively. 0.18 g/(ml of oil) of iron (III) 2-ethylhexanoate precursor and 0.23 g/(ml of oil) of titanium (IV) 2-ethylhexanoate were added to MEs based on the stoichiometry of reaction (i.e., 500 ppm NPs in final samples). Mechanism of NPs formation at the O/W interface of nanodroplet has been represented schematically in Figure 3a. The surfactant-covered oil droplets acted as a nano-reactor for the generation of NPs. Briefly, the reducing agent ions (OH^-) diffuse to the surface of nanodroplets and chemical reaction happens at the interface after collision of OH^- ions with the precursor ions. As a consequence of chemical reaction, the primary nuclei is formed which followed by growth mechanism. Finally the NPs were appeared inside the MEs which have been functionalized by stabilizer molecules.

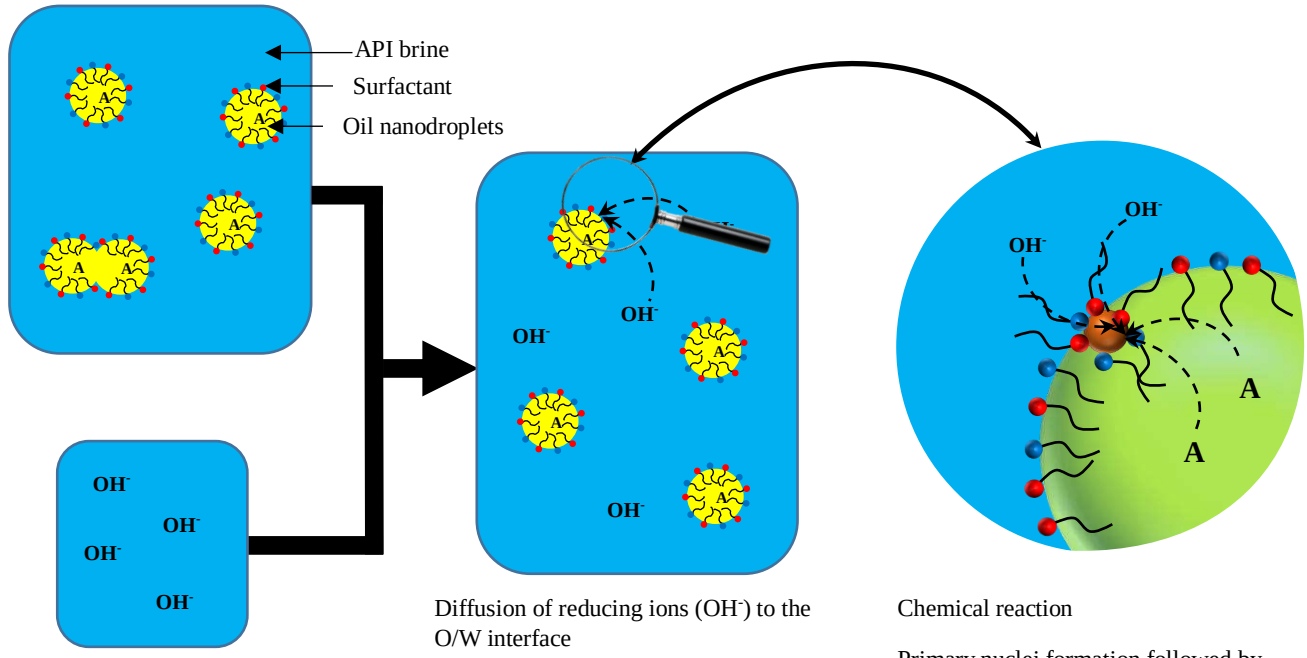

a)

b)

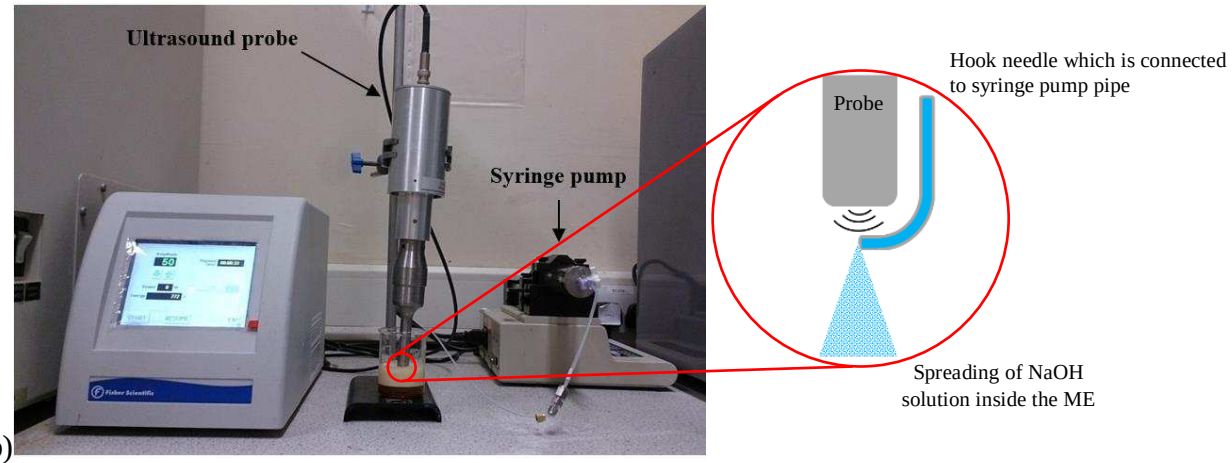

Figure 3. (a) Schematic of NPs formation inside the O/W ME, A represent the Iron (III) 2-ethylhexanoate or titanium (IV) 2-ethylhexanoate, and (b) Experimental set-up for synthesis of NPs.

Sodium hydroxide as reducing agent in brine (5wt% NaCl concentration) was injected into ME at a rate of 1 ml/min using a KDS-410-CE syringe pump. The volume ratio of NaOH solution (with a stoichiometry value):ME was considered equal to 1:30. The end of syringe pump's tube was connected to a hook needle just below the head of Ultrasound probe (Fisher scientific Ltd., Figure 3b). The droplet of NaOH solution was then spread into the ME with the amplitude of 25 out of 100 as soon as coming out from the hook needle. The ultrasonic waves also supplied the mixing energy during the reaction inside the ME media.

3. Results and discussion

3.1. Screening of microemulsions

Figure 4 illustrates the different MEs right after synthesis and after keeping them immobile for 48 hours at room temperature and 70 °C. As evident from the Figure 4, combination of J071-ND 25-12, J071-XOF 320 and O332-ND 25-12, O332-XOF 320 are more stable at HT-HS condition, which implies a synergistic effect between these groups of stabilizers. In other word, IOS and AAS have stronger synergic effect with non-ionic surfactants containing longer hydrocarbon tail. Therefore, combination of J071 and O332 with ND 25-12 and XOF 320 were selected as stable samples for further analysis (red square around them in Figure 4).

(a)

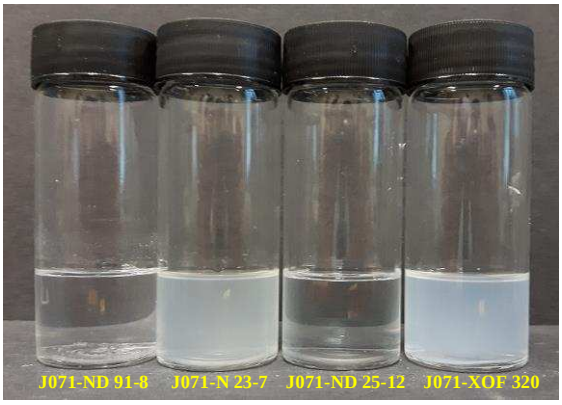

Room temperature

70 ℃ temperature

(b)

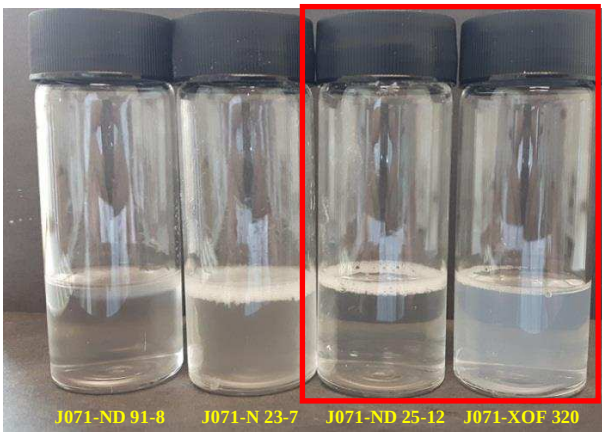

(a)

Room temperature

70 ℃ temperature

Figure 4. MEs (a) right after synthesis and (b) after 48 hours immobility (at room temperature and 70 °C).

3.2. TEM analysis of nanoparticles

The size and morphology of selected IO and TiO2 NPs were evaluated using TEM analysis after generation inside MEs. As can be seen in Figure 5, the generated NPs consist of elongated rod-shape morphology. Probably, the stabilizers molecules would adsorb to the some specific facets of primary nuclei and changed the surface growth rate of these crystal faces. The growth rate of crystal facets depend upon their surface energy and higher surface energy leads to faster growth of facet. Different growth rate of crystal facets is reason of diverse morphologes and converting of spherical primary nuclei to rod-shape NPs. The selected are electron diffraction (SAED) for the IO inside J071-XOF 320 ME and TiO2 NPs inside O332-ND25-12 ME are shown in Figure 5e, f. Diffraction rings in Figure 5e are corresponded to the d-spacing of 1.4235 Å (hkl, 221), which is in agreement with 01-072-4815 XRD reference code for tetragonal rutile morphology of TiO2. Moreover, lattice spacing (nm) of 0.2967 (220), 0.2532

(311), 0.2099 (400), 0.1616 (511) and 0.1485 (440) are observed for the IO NPs (Figure 5f), which are in agreement with the XRD data of cubic inverse spinel magnetite.

(a)

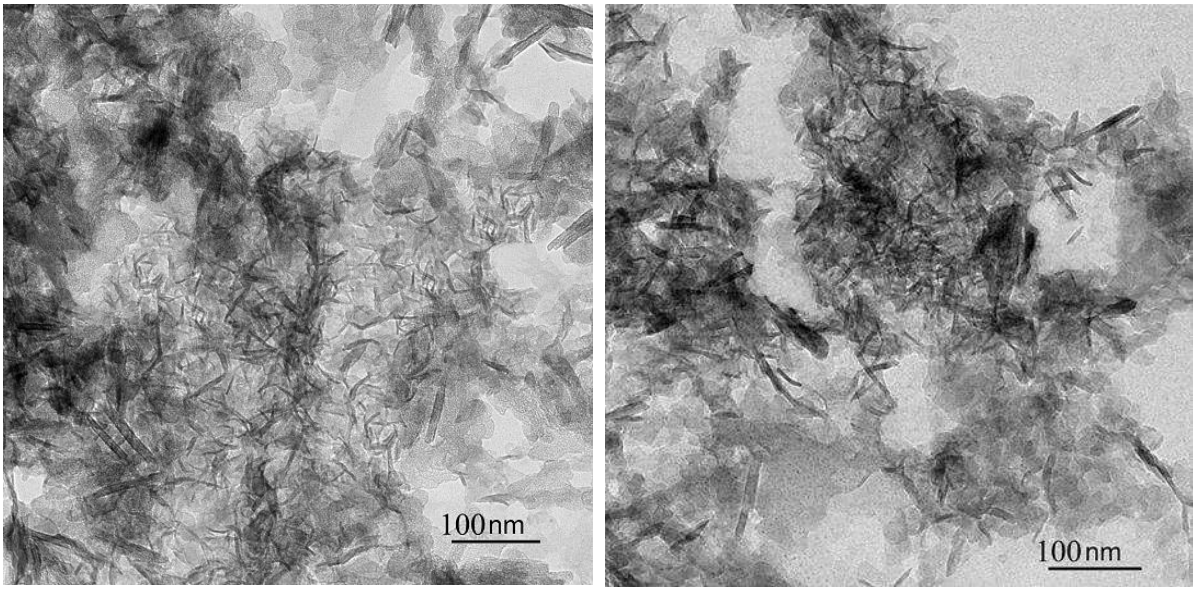

b)

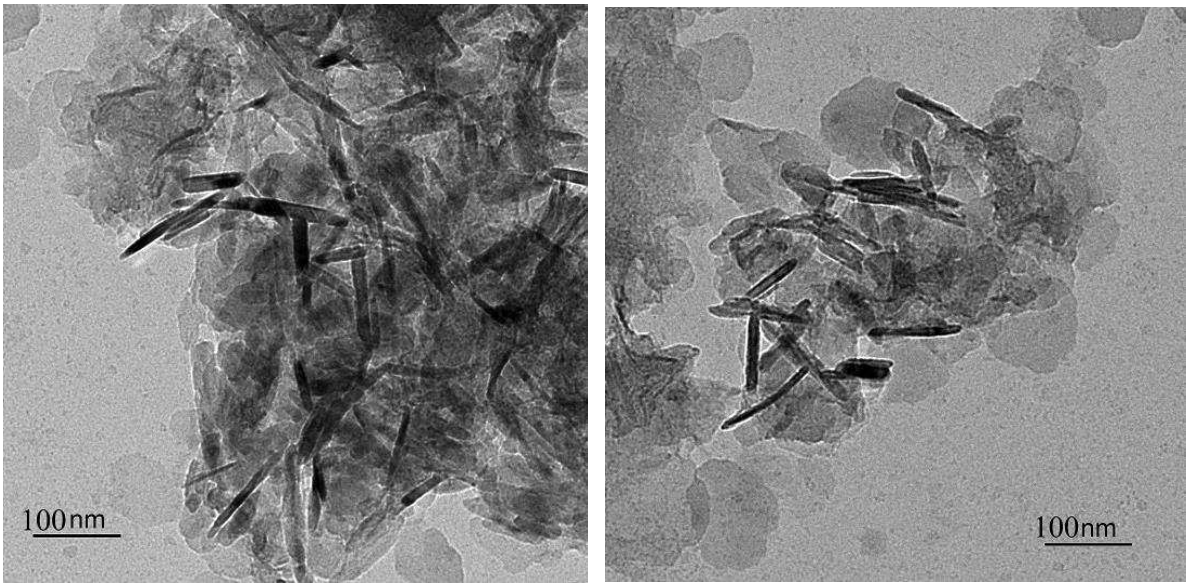

c)

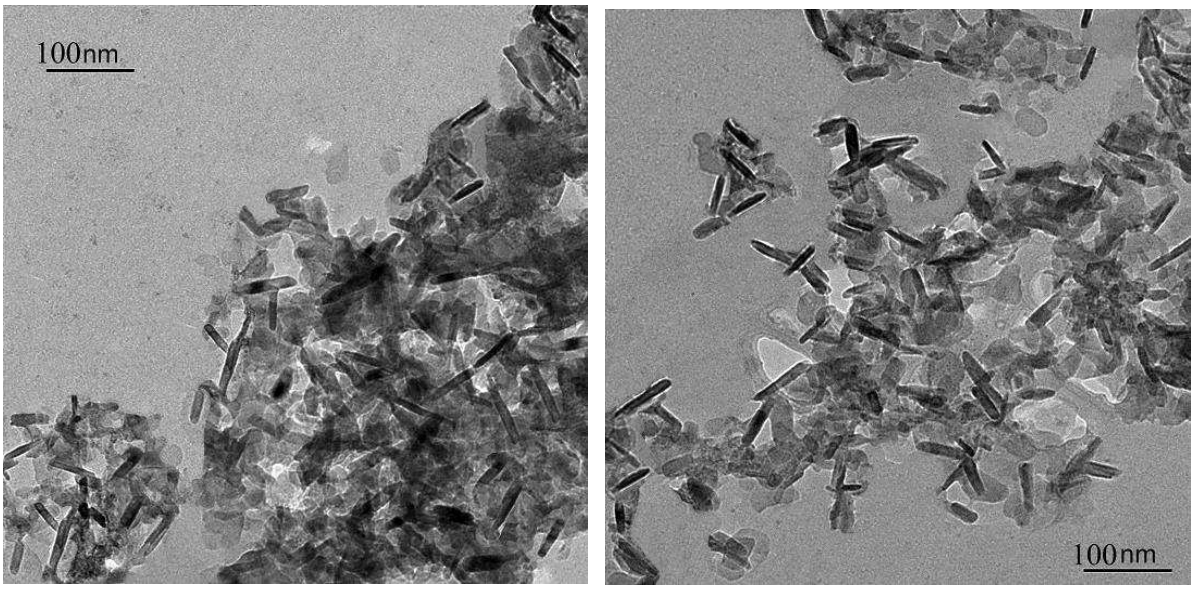

d)

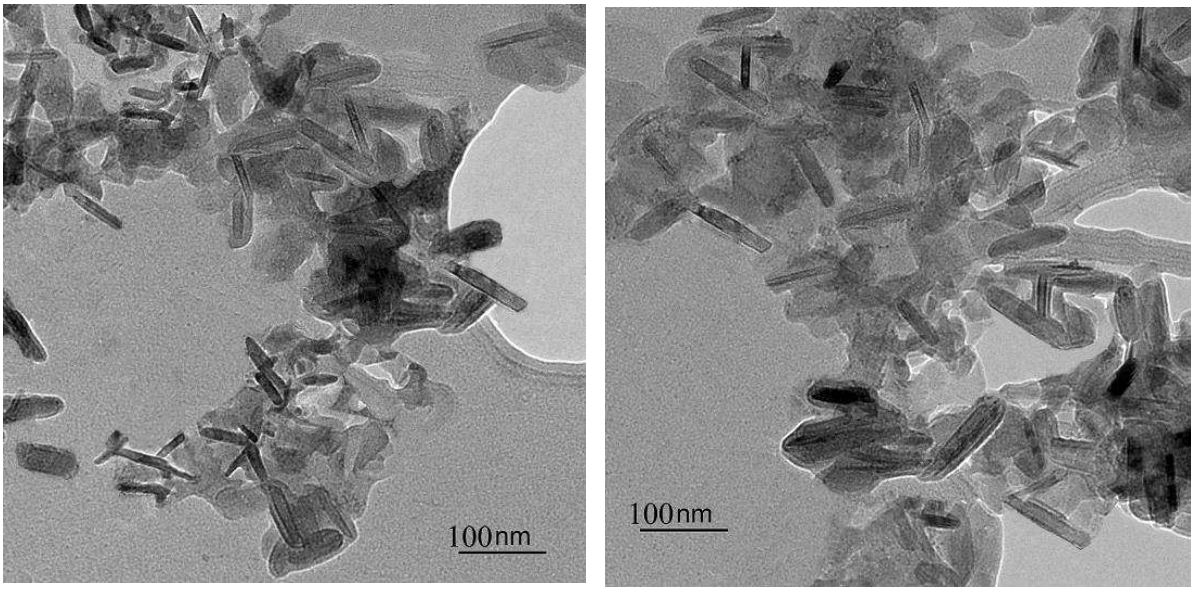

e) 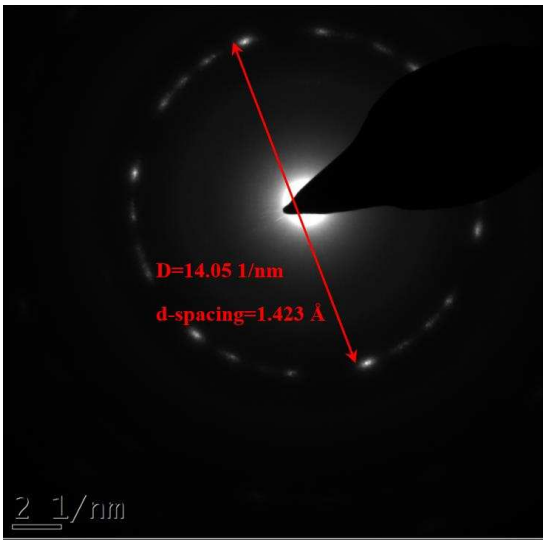

f) 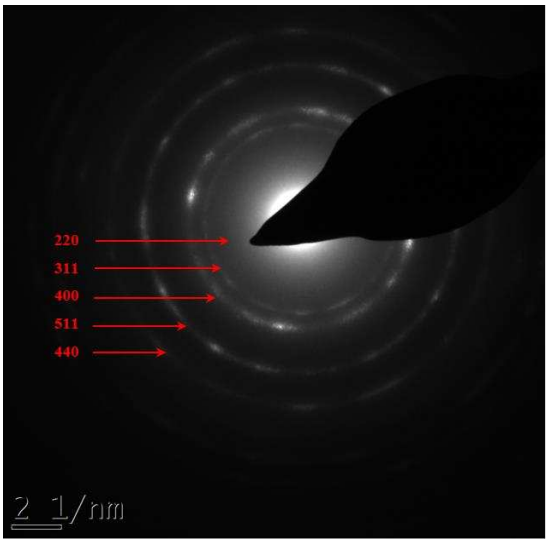

Figure 5. TEM images of IO NPs inside MEs containing (a) J071-XOF 320, (b) O332-XOF 320, and TiO_2 NPs inside MEs containing, (c) O332-ND25-12, (d) J071-ND25-12, (e) SAED of TiO_2 NPs in J071-ND25-12 ME, and (f) SAED of IO NPs in J071-XOF 320 ME.

3.3. Effect of temperature on nanoparticles formation and stability

Size distribution and aspect ratio of NPs was estimated using image processing of TEM micrographs which has been explained in our previous study (Figure 6).[28] Figure 6a and Table 2 shows the NPs size distribution synthesized at the room temperature and 70 °C. The maximum average size belongs to the formed IO NPs inside the O332-XOF 320 ME. The reason is that the larger nanodroplet's volume of O332-XOF 320 ME (Figure 6b) which provides more precursor ions during the growth step of primary nuclei.

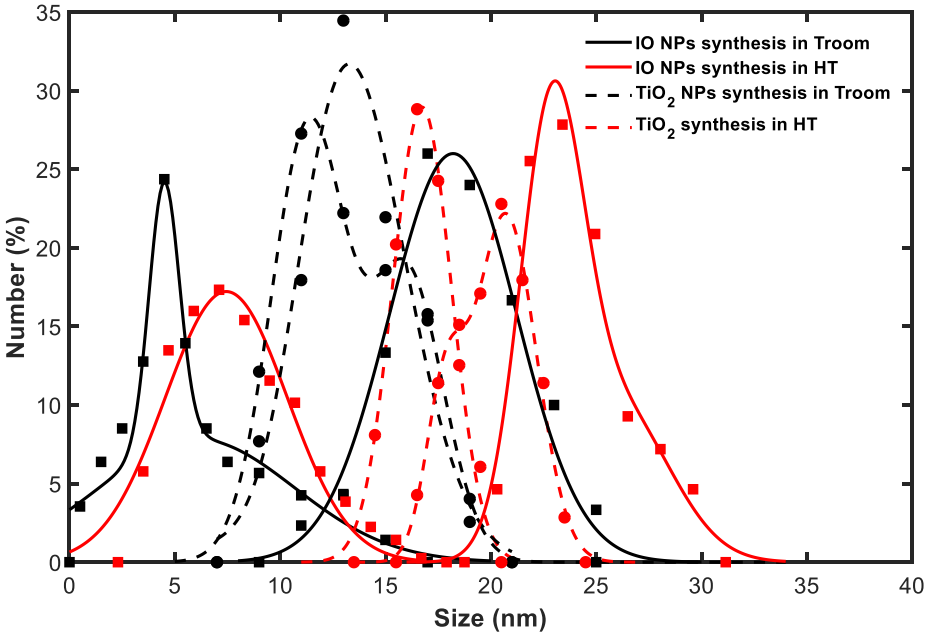
IO NPs synthesis in Troom
IO NPs synthesis in HT
TiO2 NPs synthesis in Troom
TiO2 synthesis in HT
Number (%)
Size (nm)

a)

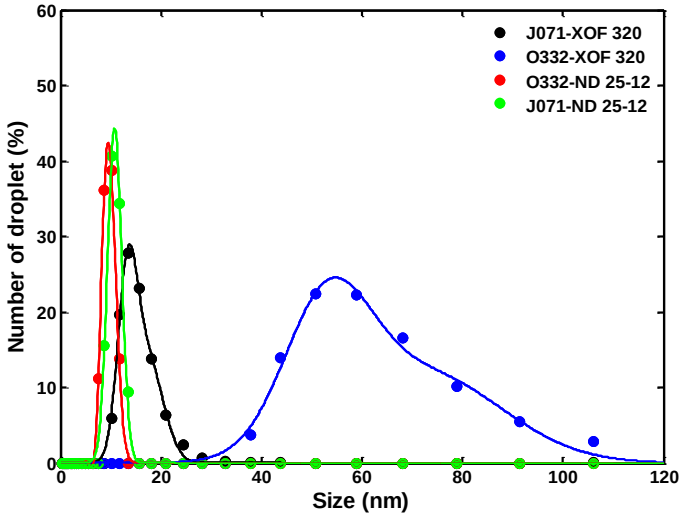
J071-XOF 320
O332-XOF 320
O332-ND 25-12
J071-ND 25-12
Number of droplet (%)
Size (nm)

b)

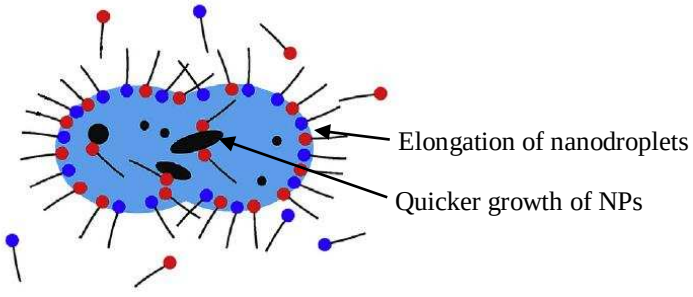
Elongation of nanodroplets
Quicker growth of NPs

c)

d)

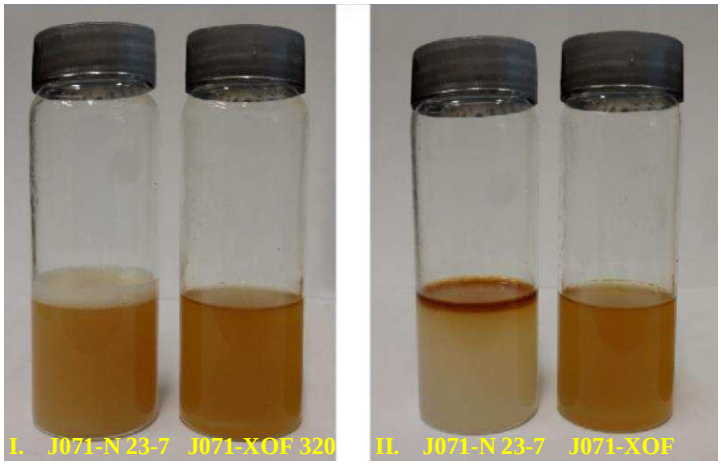

Figure 6. (a) The estimated NPs size distribution after formation at room temperature and 70 °C from the TEM images analysing for at least 100 NPs; (b) Hydrodynamic size distribution of nanodroplets for selected MEs; (c) Effect of temperature on the morphology of metal oxide NPs; and (d) stability of IO NPs inside MEs right after NPs formation (I) and after 48 hours immobility at 70 °C (II).

Table 2. Average size and aspect ratio of metal oxide NPs after formation in various MEs.

		IO NPs		TiO_2 NPs	
Sample / Temperature		**J071-XOF 320**	**O332-XOF 320**	**O332-ND25-12**	**J071-ND25-12**
Room temperature	Average size	5	18	13	14
	Aspect ratio	4.96±1.5	6.12±2.3	5.09±0.8	5.36±1.3
70 °C	Average size	8	24	17	19
	Aspect ratio	6.03±0.7	7.22±2.1	6.61±0.5	6.53±2.0

Increasing the temperature promoted the aspect ratio and average size of rod-shaped NPs. The reaction rate for NPs generation is higher at elevated temperature, which promote the growth of crystalline structure of NPs compare to room temperature. The higher temperature also increase the vibration and separation of surfactant molecules at the O/W interface which reduce the rigidity of interface and facilitate deformation of nanodroplets in shear direction (Figure 6c). The transient deformation of droplets in specific direction would has a positive effect on growth of elongated particles in same direction.[28] Similar to the nanodroplets, functionalizing

of NPs with surfactants blend would improve their stability in harsh environment. The stability of NPs inside the MEs was evaluated visually after formation of NPs inside MEs. IO NPs-MEs including J071-N 23-7 and J071-XOF 320 blends have been selected as representative for stable and unstable formulation in harsh environment. Figure 7d shows the samples right after NPs formation and after keeping them immobile for 48 hours at 70 °C.

3.4. Effect of salt and nanoparticles on interfacial tension

The transient surface tension of surfactant solutions containing individual or surfactants blend (equal amount of anionic and nonionic type) is shown in Figure 7. Generally, presence of salt in surfactant solution reduce the surface tension. The degree of surface tension reducing depends on type and concentration of both surfactant and salt.[29] The main reason for such an observation is attributed to the effect of electrolytes on electrical double layer (EDL) around the hydrophilic head of surfactant molecule. Electrolytes could reduce the thickness of the ionic atmosphere around hydrophilic head of surfactant molecules, which promote the aggregation of surfactant molecules. As another consequence, the rate of surface adsorption for surfactant molecules at the air-water is increased with the addition of salt.[30,31] According to Figure 7a, the effect of salinity on surface tension reduction is higher for anionic surfactant in comparison to nonionic one (ND25-12 and XOF 320) due to higher degree of EDL compression.

a) b)

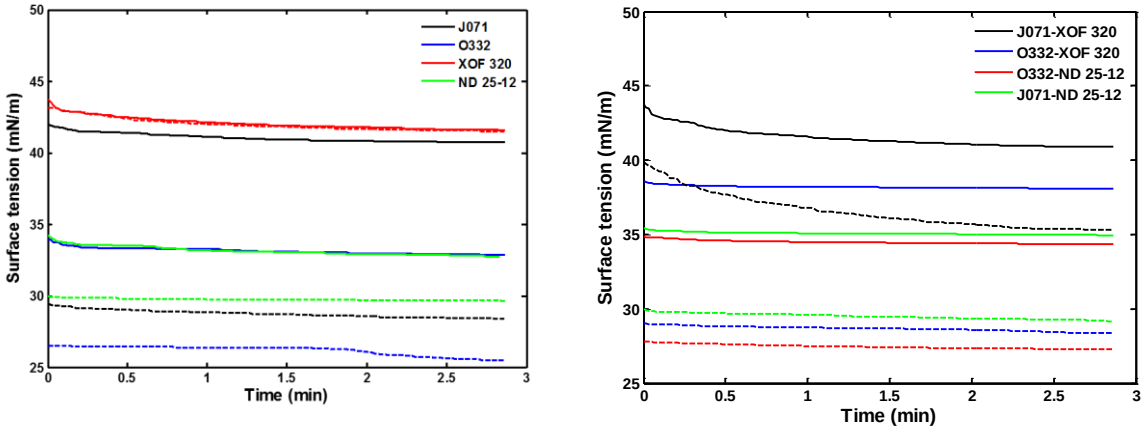

Figure 7. Surface tension of a) individual surfactant and b) surfactants blend in (solid line): deionized water and (dashed line) API brine (total surfactant concentration of 0.01 g/ml).

The IFT between surfactant solutions containing individual or surfactants blend (equal amount of anionic and nonionic type) and oil phase is represented in Figure 8. Similar results can be

observed for decreasing of IFT in the presence of salt. Sodium chloride, as a lyotropic salt, reduce the solubility of surfactant molecules inside water and force them to move from inorganic phase to the organic phase. [32] As a result of surfactant movement, the number of molecules at O/W interface is increased and IFT is decreased.

a) b)

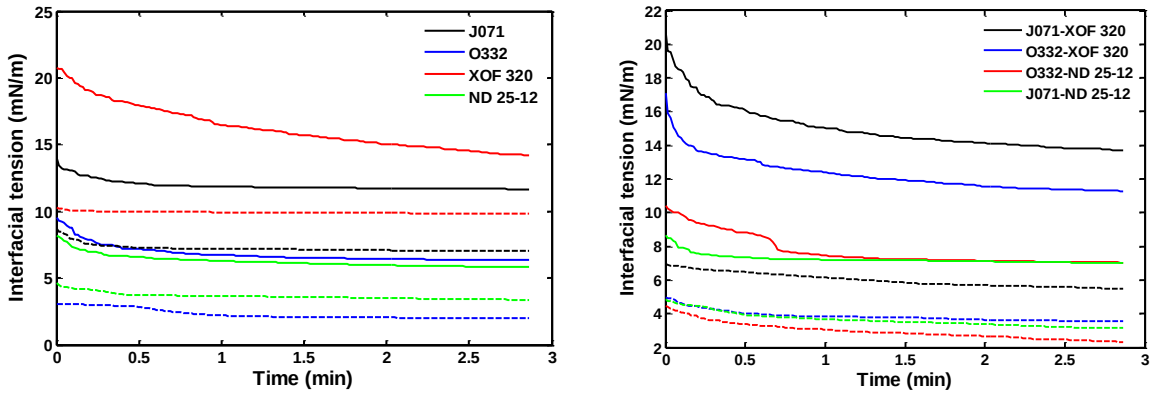

Figure 8. IFT of a) individual surfactant and b) surfactants blend in (−): deionized water and (--) API brine (total surfactant concentration of 0.01 g/ml).

The effect of NPs on IFT value of emulsions depends on behaviour of NPs in ternary system of surfactant-brine-oil which is not predictable. According to the literature, many parameters including hydrophilic/hydrophobic tendency, concentration and surface charge of NPs, surfactant polarity could influence the O/W IFT in presence of surfactant/NPs. There is a controversy between researchers about the effects of NPs on O/W IFT. A group of researcher reported that the presence of NPs reduce the IFT, while the other group observed the increasing of IFT value. The results of some outstanding research form both sides are briefly reviewed here. Vatanparast et al.[33] reported that the reducing of IFT for ternary system of n-heptane-water-anionic surfactant (sodium dodecyl sulfate or dodecyl benzene sulfonic acid) in the presence of hydrophilic silica NPs. According to the results, the diffusion of molecules through the bulk to the interface is quicker at higher concentration of NPs. Therefore, a shorter time taken for the surface tension to reach an equilibrium in presence of NPs. Saien and Bahrami[34] observed a similar conclusion for the impact of silica NPs on IFT of water-normal hexane-sodium dodecyl sulphate (SDS) system. They also investigated the effect of NPs size (11-14, 20-30 and 60-70 nm) on IFT values of ternary system. According to their results, the IFT reduction increased once the smaller silica NPs were mixed in solution. The reason is attributed to higher chance of the smaller particles to displace at the O/W interface.

Biswal and Singh[35] studied the effects of several types of NPs (different surface charge) and oil phase on the O/W IFT in presence of nonionic Tween 20 surfactant. They concluded that presence of NPs in emulsion, irrespective of type of particles, had adverse impact on ability of surfactant molecules in reducing of IFT. They stated that the affinity of surfactant to the surface of NPs was the main reason for such observation. Adhering of surfactant unto the surface of NPs would disrupt the movement of molecules from the bulk of solution to the W/O interface. Therefore, the number of molecules at the interface is reduced that means reduction of IFT. In another study, Whitby et al.[36] investigated the effect of hydrophilic silica NPs (1 wt%) on IFT of octadecyl amine-hexane-water system. According to their results, the IFT of emulsion could increase in presence of NPs which considerably depends on concentration of surfactant. At low concentration of surfactant, any significant change was not observed for IFT, while much higher IFT values were measured by increasing the concentration. They proposed that a packed surfactant layer would be formed at the O/W interface at high concentration of surfactant. In presence of NPs, a fraction of functionalized particles attached to the interface and altered the saturated surfactant layer. Therefore, higher IFT was observed in presence of NPs due to replacing of surfactant molecules with NPs.[36] The equilibrium IFT data of surfactants mixture in the API brine (micelles form) and MEs (before and after NPs generation) is presented in Figure 9a. Obviously, the IFT is increased for NPs-MEs in compare to MEs. Presumably, as suggested by Biswal and Singh [35], the number of surfactant molecules at the O/W interface will be reduced after adsorption on surface of NPs (move by Brownian motion inside the ME). Therefore, staying a major fraction of surfactant molecules in the bulk of solution reduce the availability of stabilizer molecules to move to the O/W interface (Figure 9b).

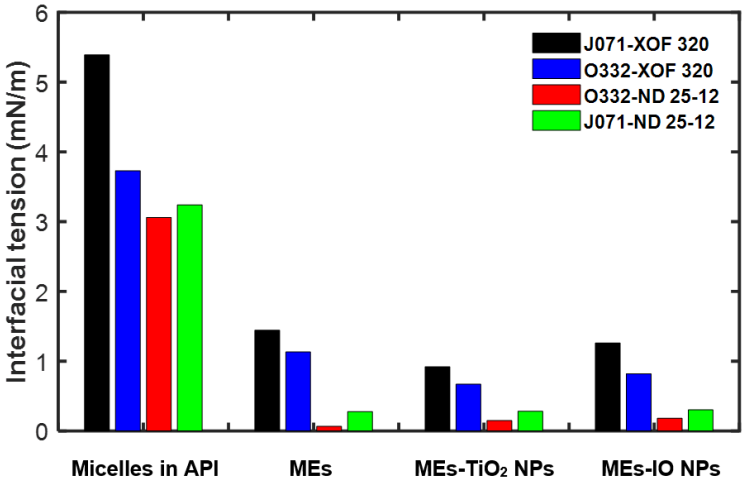

(a)

(b)

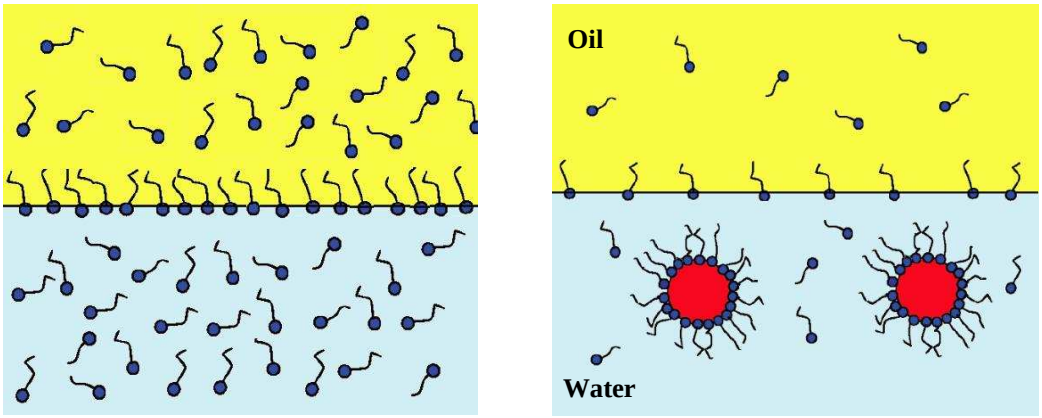

Figure 9. (a) IFT of API brine and microemulsion (before and after NPs generation) (b) available number of surfactant molecules to transport to the interface in absence and presence of NPs.

3.5. Effect of nanoparticles on rheological behaviour

Figure 11 represents the viscosity of surfactant solution in deionized water and API brine as a function of shear rate (du/dy).

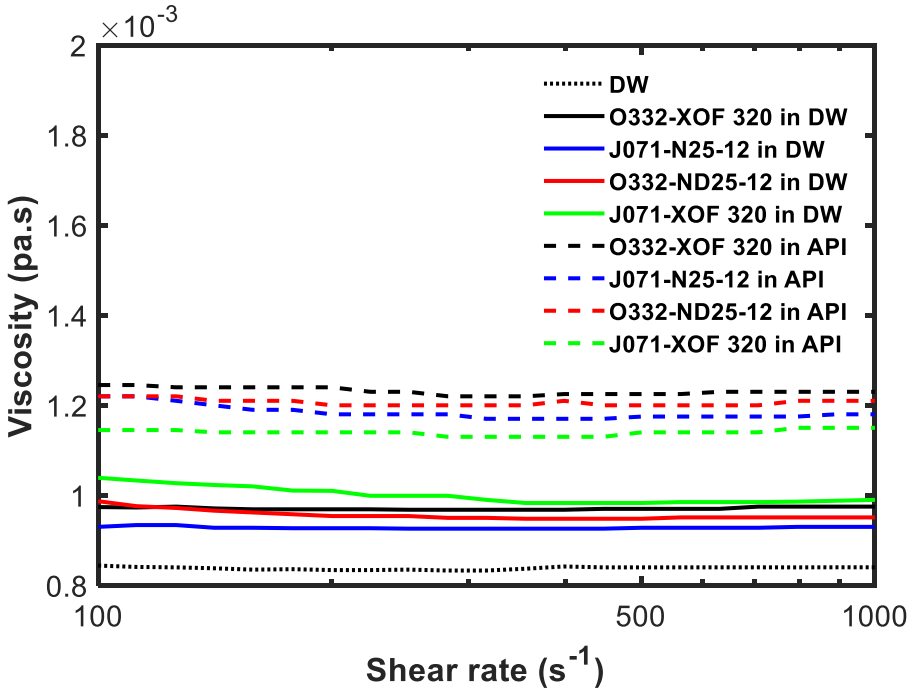

Figure 10. Viscosity curve of surfactants blend dispersion in deionized water (DW) and API brine (total surfactant concentration of 0.015 g/ml).

Surfactants blend increased the viscosity of solution relative to pure water by formation of micelles, which act as a disperse phase in aqueous solution. Moreover, the viscosity of

surfactants blend in API brine is higher than de-ionized water. Previous researchers proposed two main reasons for increasing of viscosity in the presence of salt: Brownian motion and Debye-Huckel effect of ions in water.[37,38] Monovalent and divalent ions could treat as particles, which carry momentum across the liquid. Moreover, according to Debye-Huckel theory, there is a certain resistance to shear due to the presence of ionic interactions which leads to increment of viscosity. Another important reason for the increasing of viscosity might be due to growth of micelles size in API brine which resist against shear forces. The ions in API brine rise the aggregation number of micelles via diminishing the effective polar head area of surfactant molecules in a micelle.[39]

Figure 12 represents the viscosity of MEs and surfactant solution in API brine. As evident from the figure, the surfactant solution shows a Newtonian plateau behaviour in the total range of shear rate.

Cheng et al.[40] assessed the dynamic viscosities of Triton X-100 and SDS solutions at three different temperatures and showed that both surfactants solution have Newtonian fluidic behaviour. Their rheology analysis confirmed the Newtonian behaviour of surfactant solution even at the surfactant concentration much higher than critical micelle concentration (e.g. 1203 ppm for Triton X-100). Other studies have also reported that there is no significant change in the Newtonian behaviour of surfactant solutions before formation of micellar structure (dilute concentration).41,42 However, formation of micellar structures has a considerable effect on rheological behaviour of surfactant solution.[43] Pal et al.[44] studied the viscosity of non-ionic gemini surfactants and observed shear thinning behaviour (pseudoplastic) for surfactant solution particularly at low shear rate (150 s^{-1}).They justify the observation by helping of order-disorder transition (ODT) theory. In this way, the viscosity reduce by increasing the shear rates due to micelles structural change upon transition from an ordered to disordered state.

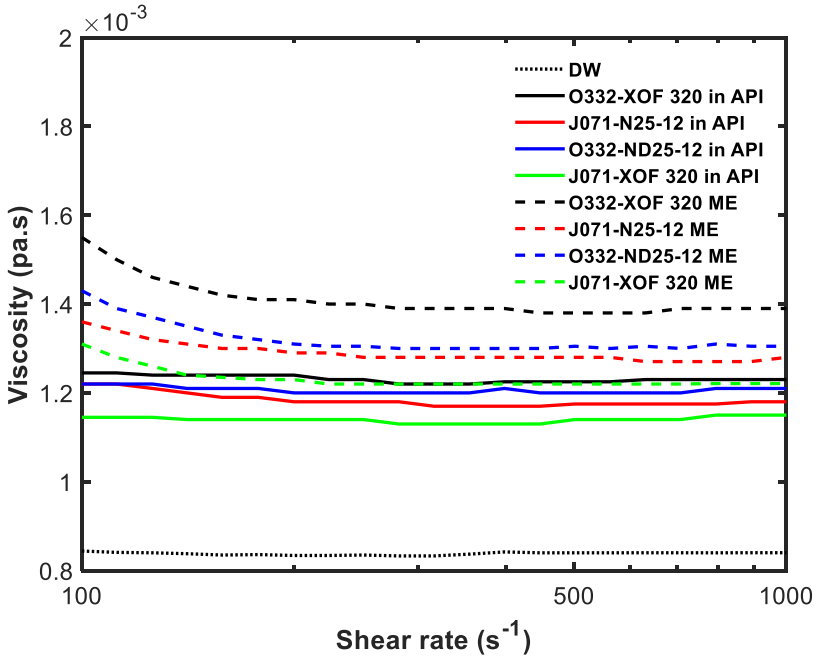

Figure 11. Viscosity curve of MEs and surfactants solution in API brine (total surfactant concentration of 0.015 g/ml).

There are several well conducted studies on the rheological behaviour of MEs particularly for EOR applications.[10,45,46] According to Figure 11, the Newtonian behaviour of surfactants solution changes to non-Newtonian shear thinning behaviour for MEs which is in a good agreement with observation of other reserachers.[47] The oil nanodroplets are obstacles against the shear force which improve the viscosity of MEs in compare to surfactants blend at similar type and concentration of surfactants. However, at higher shear rate, the droplets arranged along with flow stream line and shear thinning behaviour is observed.[48] Figure 12 shows the viscosity for MEs before and after formation of NPs. Formation of NPs significantly improve the shear-thinning pseudoplastic behaviour of MEs. The NPs would form a network across the ME and improve the shear-thinning behaviour. Moreover, NPs could adsorb at the interface of oil nanodroplets and reinforce their stability. By increasing the shear rate, viscosity started to upturn quickly due to separation of NPs from interface and destroying the network across the ME. Maurya and Mandal[10] reported the similar shear thinning trend for silica NPs inside emulsion of SDS. However, a shear thickening behaviour was observed across the entire range of higher shear rates. They concluded the droplets packed closer together at higher shear rates that leads to formation of a new thickening microstructure.[10]

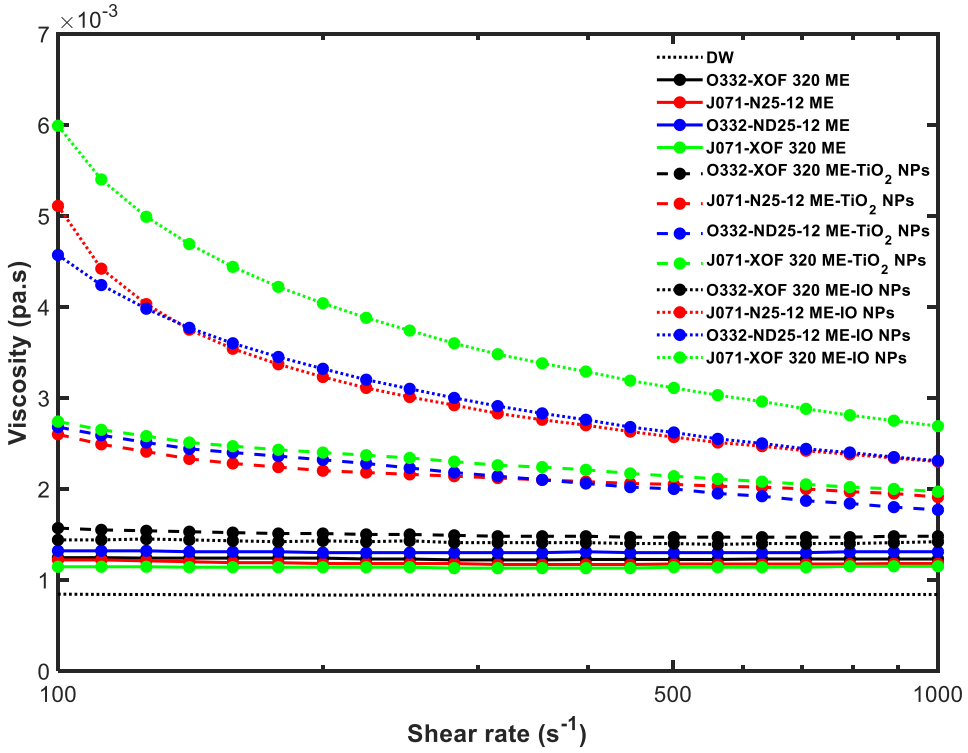

Figure 12. Viscosity curve of microemulsions before and after nanoparticles formation.

Figure 13 represents the storage modulus (G′) and loss modulus (G″) of MEs before and after formation of NPs in log-log scale, separately. Water is a Newtonian fluid at 25 °C with G′=0 Pa and G″=μω which was specified in Figure 13 by black line. Generally, both G′ and G″ increase with frequency in the whole range, with a certain slope depending on the type of suspension. Increasing of the solid-like behaviour of MEs can be clearly observed in Figure 13 after formation NPs. The stronger solid-like behaviour for ME samples including IO NPs confirms higher physical interaction between IO NPs and oil nanodroplets. The information about viscoelastic properties of micro- and nano-emulsions are very limited in the literature for comparison. Our results showed similar characteristics to that of Kumar and Mandal, who reported an increase of G′ (storage modulus) and G″ (loss modulus) values with increasing angular frequency (rad/s).[45]

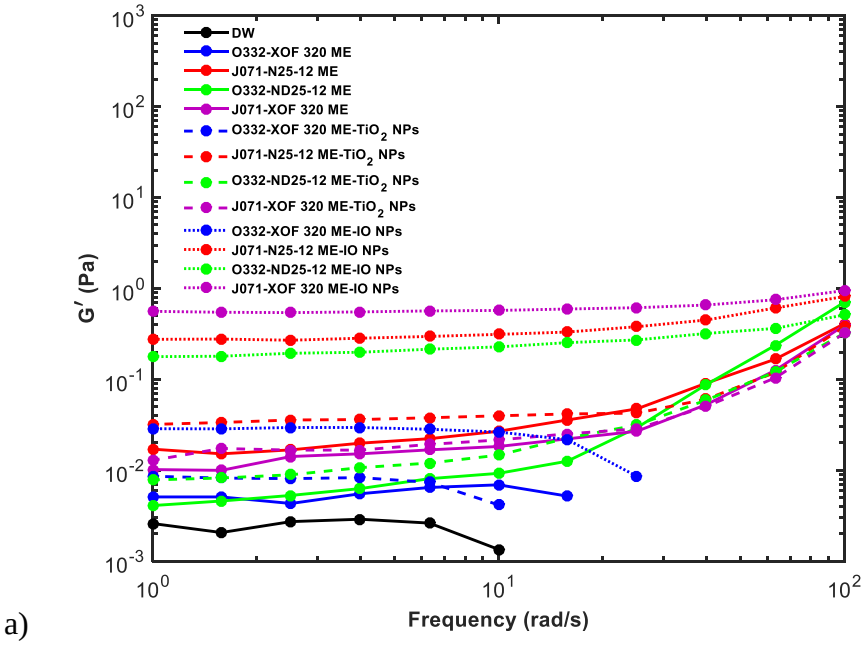

a)

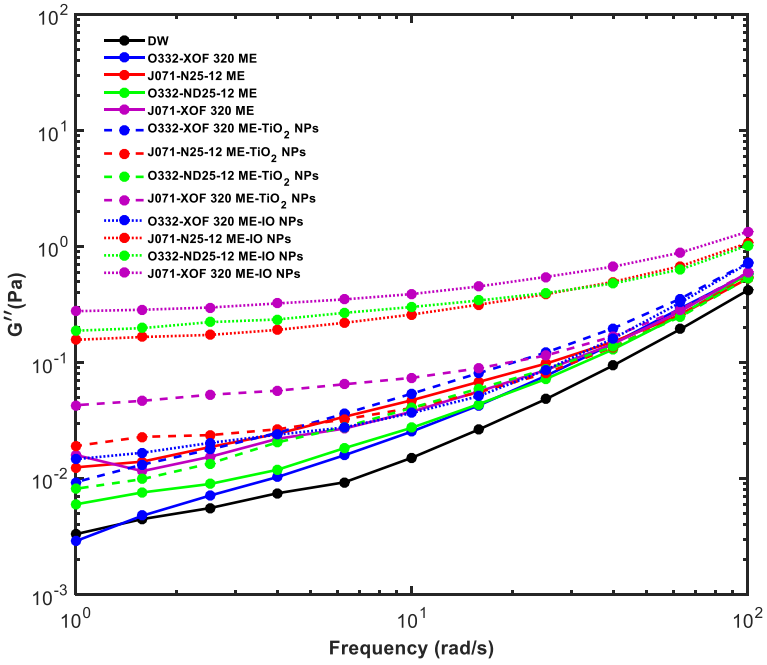

b)

Figure 13. (a) Storage modulus (G′) and (b) loss modulus (G″) of different samples.

Both storage modulus (G′) and loss modulus (G″) of MEs and IO NPs MEs are illustrated in Figure 14. The G′ values of the MEs in absence of NPs are smaller than G″ values at whole frequency range, suggesting the liquid-like behaviour (viscous nature) of MEs. After formation of NPs, the G′ values are initially greater than G″ indicating viscoelastic behaviour of IO NPs ME solutions. However, G″ values became higher than G′ for frequencies after crossover point

implying the domination of liquid like properties of the suspension. In this sense, the transient form viscoelastic to viscous nature probably is due to separation of NPs from surface of nanodroplets at high frequency. Similar results were observed by other researchers for the effect of NPs on the rheological behaviour of polymeric solutions and emulsions.[14,49] The authors think that there is a remarkable interaction between IO NPs with alcohol alkoxy sulfate surfactant for improvement of viscoelastic behaviour of MEs. The interaction between NPs and surfactants could be investigated by molecular dynamics (MD) simulation, which is beyond the scope of current study.

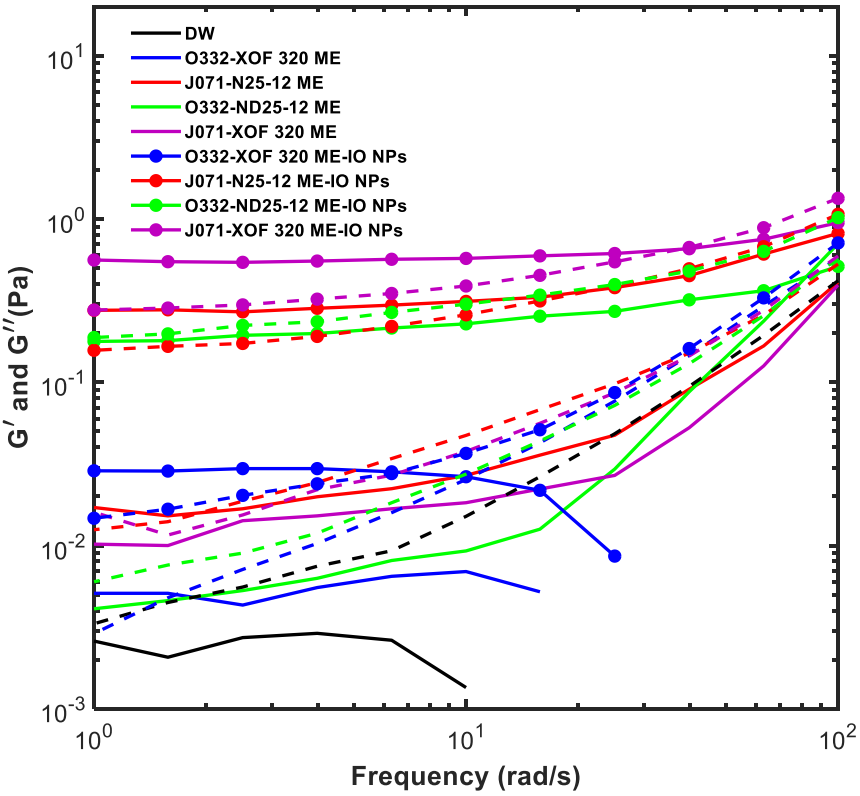

Figure 14. Storage modulus, G′ (solid line), and loss modulus, G″ (dashed line), of MEs and MEs containing IO NPs.

3.6. Phase behaviour of surfactant mixture

Phase behaviour analysis was performed to determine the type and quality of ME formation after contacting with oil bank. Glass pipette method was used to evaluate the phase behaviour

of whole selected MEs.[50,51] One ml of ME and one ml of crude oil were put in a long glass pipette with 3mm internal diameter, then sealed and mixed end-to-end in a rotary mixer, at room temperature for 1 hour. All pipettes were kept at 70 °C in an oven for 3 weeks to reach to equilibrium (Figure 15a). The pipettes were removed periodically from the oven a few times during the experiment period and were briefly mixed end-to-end manually. According to Figure 15a, Winsor type III (bicontinuous oil/water phase) was formed for O332-ND25-12 ME and J071-XOF 320 ME while Winsor type I was formed for J071-ND25-12 ME. On the other hand, the viscous emulsion phase was appeared for O332-XOF 320 ME. Formation of viscous phase can be easily detected by rotating glass end-to-end and remaining stationary. Formation of viscous phase inside the glass tube prevented mixing of water and oil phases (Figure 15b). Generally, the viscous structure do not transport well in porous media under low pressure gradients, and often result in high surfactant retention and low oil recovery.[51,52] Evidences such as larger average droplets size and formation of viscous phase imply a weak synergistic effect for O332-XOF blend in compare to other ones. To sum up, identification and screening of synergic effect between surfactants blend is a vital step before utilizing of blend for chemical flooding process including surfactant solution, ME and ME-NPs for EOR application.

a)

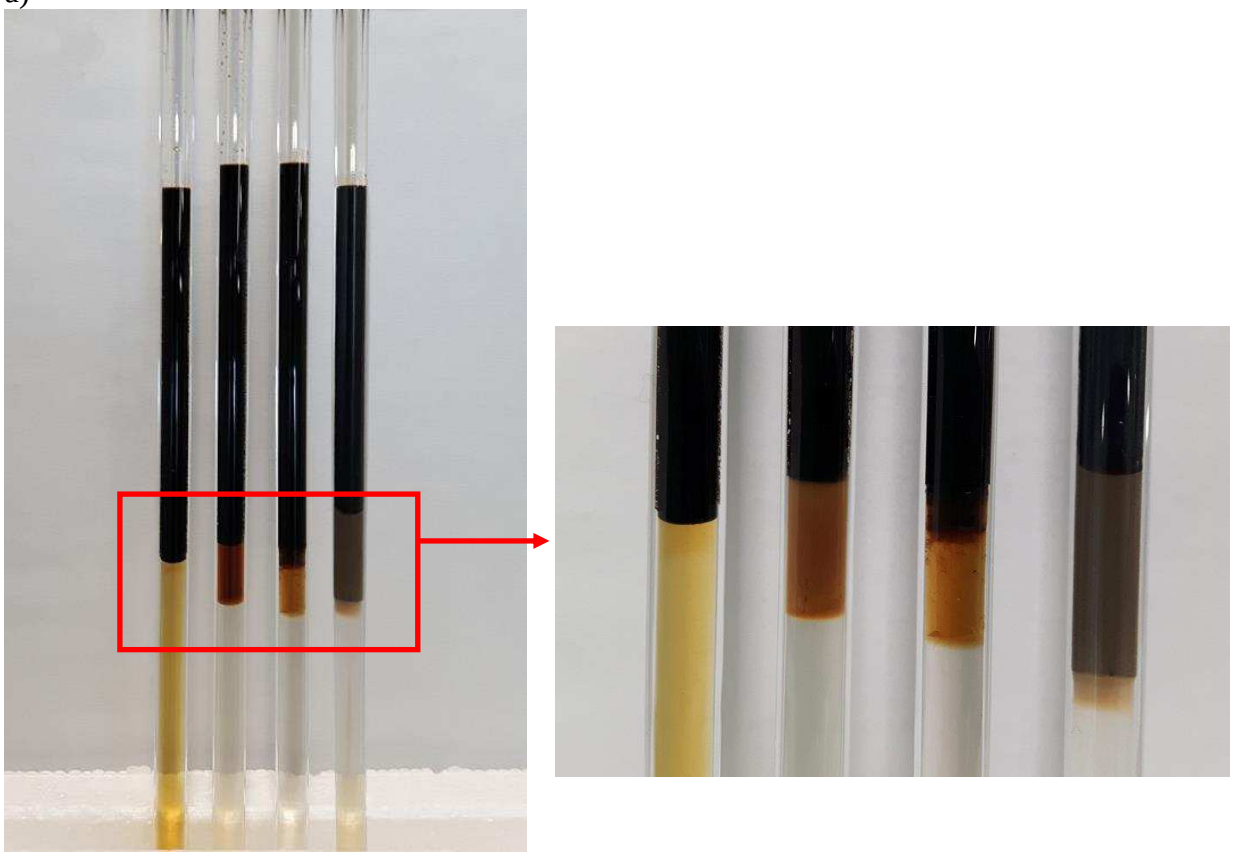

b)

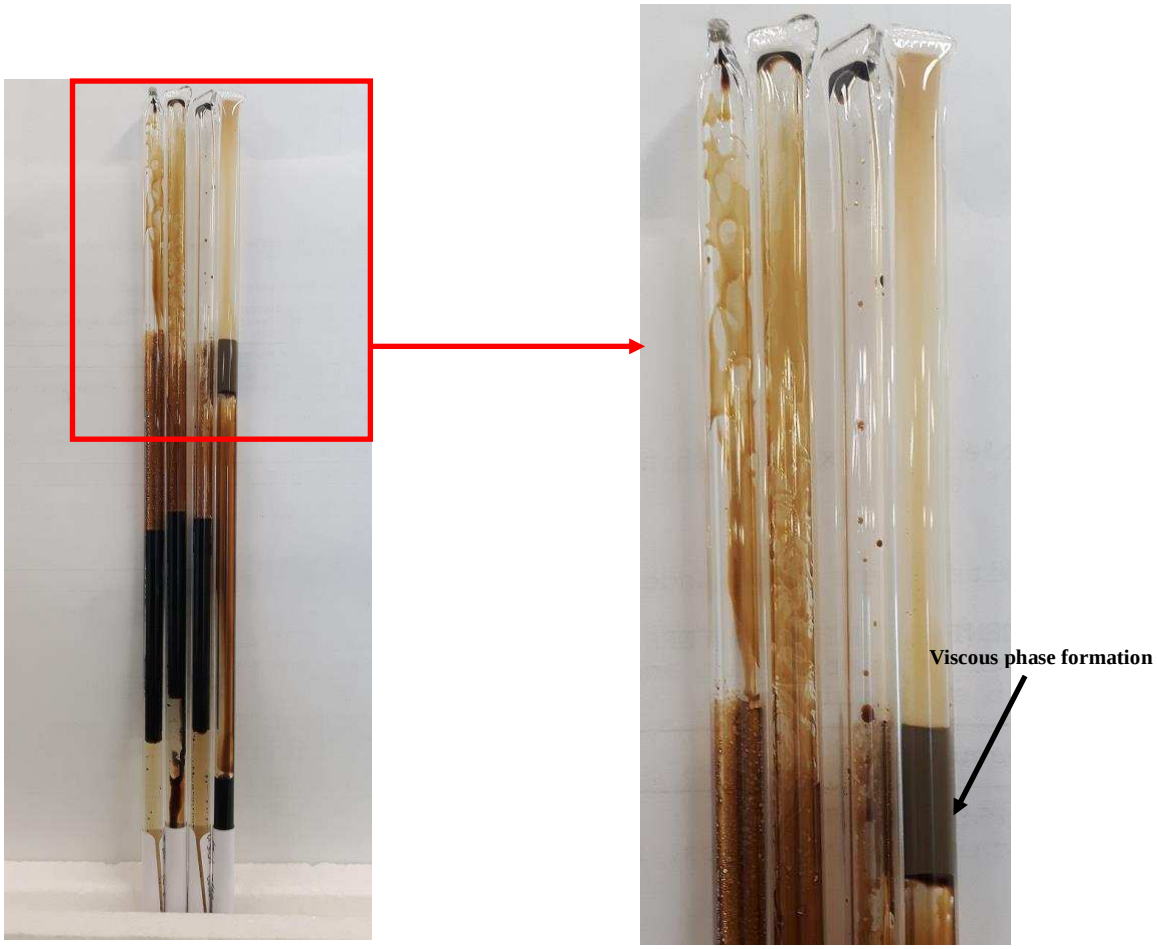

Figure 15. (a) Phase behaviour results of MEs with crude oil at 70 ºC after 3 weeks (b) rotating glass tube end to end and remaining stationary.

3.7. Enhanced oil recovery

Figure 16 illustrate the nanofluidic chip during the injection of different slugs. The proper slugs were selected according to the above analysis results. The oil displacement was estimated equal to 69.8, 71.6, 73.5 and 76.9% after injection of API brine, O332-ND 25-12 ME, O332-ND 25-12 ME-TiO_2 NPs, and O332-ND 25-12 ME-IO NPs slugs, respectively. According to observation, the formation IO NP increase the oil displacement about 5.3 and 7.1 in compare to the API brine and ME injection.

(a) API brine flooding

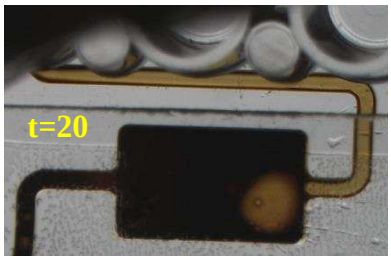

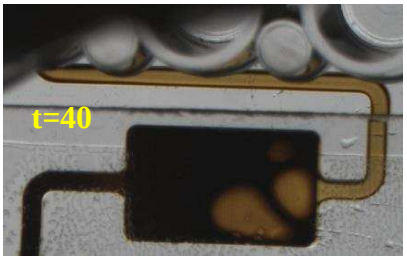

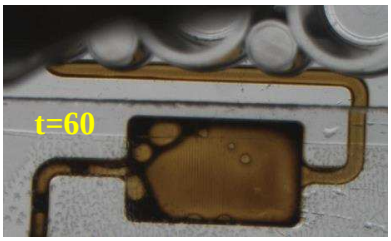

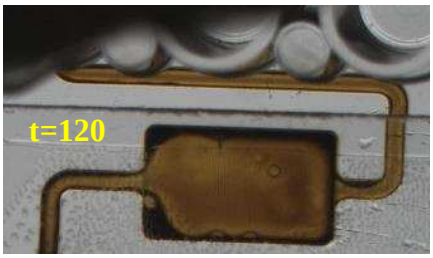

(b) O332-ND 25-12 ME flooding

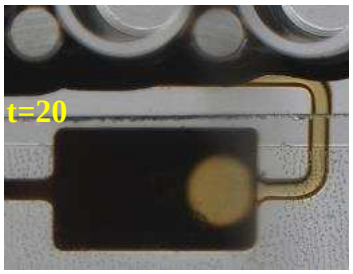

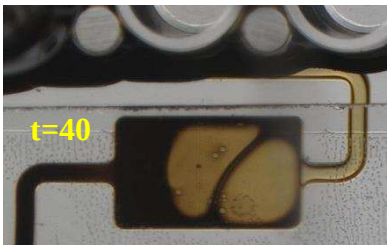

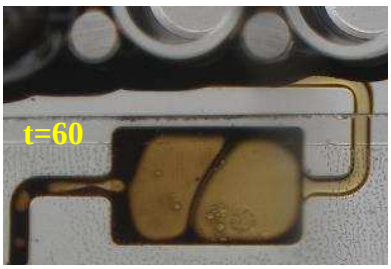

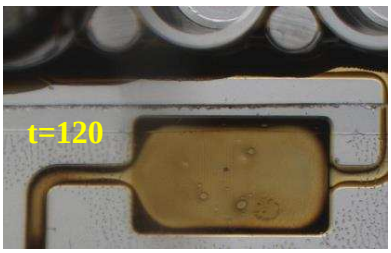

(c) O332-ND 25-12 ME-TiO_2 NPs flooding

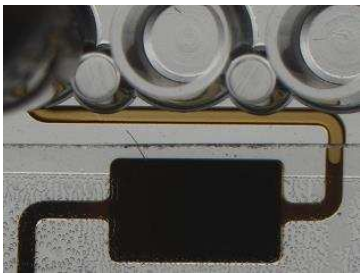

OOIP=100% (t=0 min)

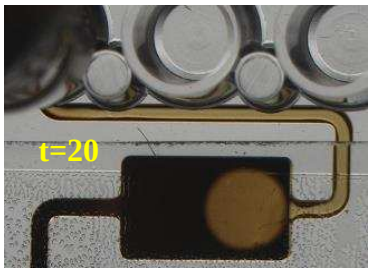

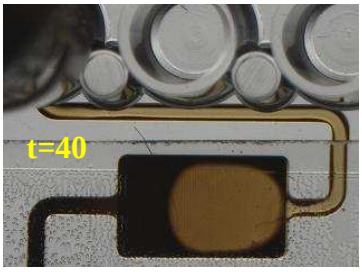

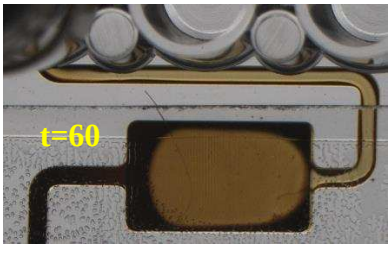

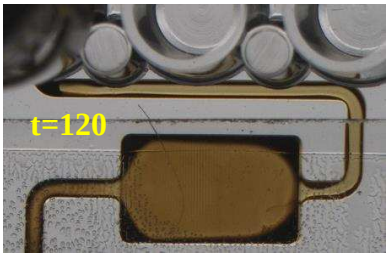

(d) O332-XOF320 ME-IO NPs flooding

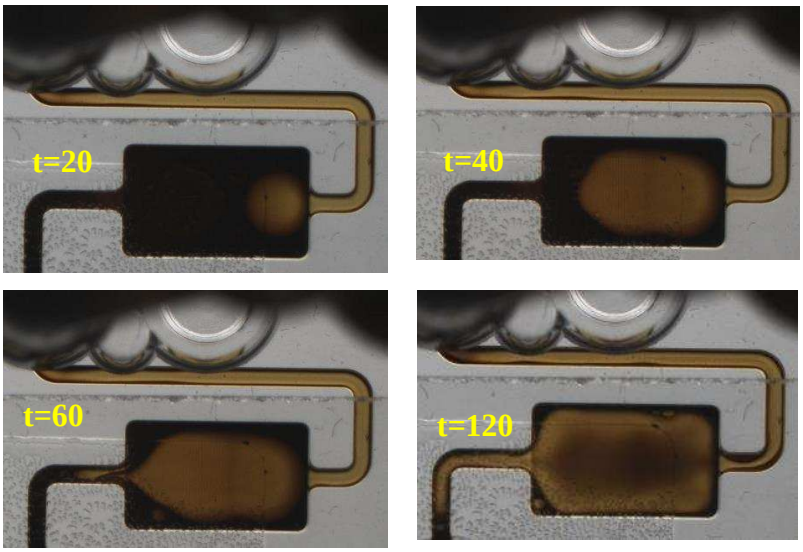

Figure 16. Optical micrographs of crude oil displacement after injection of (a) API brine, (b) O332-ND 25-12 ME solution, (c) O332-ND 25-12 ME-TiO_2 NPs flooding, and (d) O332-ND 25-12 ME-IO NPs flooding.

NPs could assist EOR via several proposed mechanisms including IFT reduction, increasing the mobility ratio, wettability alteration and log jamming inside the porous media.53 The cycloolefin copolymer microchip was selected in this study to minimize the effect of wettability alternation during the flooding test. The selected microchip is highly hydrophobic (oiliphilic) and any sensible change was not observed for contact angle of oil droplet on top of microchip in API or NPs in ME environment. The effect of NPs formation on IFT has been fully described in Section 3.4, which showed an increase of IFT after NPs formation inside ME. Therefore, the wettability modification and reduction of IFT are not the possible mechanisms for improvement of oil displacement in the presence of NPs. It seems that the effect of NPs on rheological behaviour is the main mechanism, which modify the mobility ratio between aqueous and crude oil bank, leading to improved oil recovery efficiency.

4. Conclusions

This work develops a new method of forming nanoparticles in microemulsions to improve their stability under harsh conditions. The screening of synergistic effect between commercial surfactants was firstly performed for synthesis of stable MEs in a harsh environment. The iron

oxide and titania oxide NPs were then synthesized inside the selected stable MEs. More specific points can be drawn as follows:

-Metal oxide NPs with elongated rod morphology were formed inside the MEs media in high salinity-high temperature. The appearance of rod morphology is attributed to different growth rate of crystal facets after adsorption of surfactant molecules on surface of facets.

-After formation of NPs inside MEs, the IFT between MEs and oil phases was increased. The reason is due to the adsorption of a fraction of surfactants molecules on NP's surface. The NPs move by Brownian motion inside the MEs and therefore the number of surfactant molecules at O/W interface is reduced.

-Unlike to the effect of NPs on IFT, the viscosity and viscoelastic properties of MEs were improved after the formation of NPs in MEs. Newtonian behaviour of pure surfactant solution was converted to non-Newtonian shear thinning behaviour in form of ME. Moreover, the formation of NPs improved the shear-thinning behaviour of MEs and boosted the solid-like behaviour.

-The results of microfluidic flooding showed the increase of oil displacement after the formation of NPs inside MEs. The main reason for increasing of oil recovery efficiency was the improvement of the rheological behaviour of ME, which could have a great potential for EOR applications.

■ Author information

Corresponding Author: Dr Ehsan Nourafkan
Email: Enourafkan@lincoln.ac.uk
Corresponding Author: Prof Dongsheng Wen
Email: D.Wen@leeds.ac.uk and D.Wen@buaa.edu.cn

Notes

The authors declare no competing financial interest.

■ Acknowledgments

The authors would like to thank Paul Kunkeler (Shell Ltd.) and Timur Zaynetdinov (Huntsman Ltd.) for generously providing us with their products. This work is supported by European Research Council Consolidator Grant (Grant number: 648375).

■ References

[1] McClements D.J. Nanoemulsions versus microemulsions: terminology, differences, and similarities, Soft Matt. **2012**, 8, 1719-1729.

[2] Nourafkan, E. Gao, H. Hu, Z. Wen, D. Formulation optimization of reverse microemulsions using design of experiments for nanoparticles synthesis, Chem. Eng. Res. Des. **2017**, 125, 367-384.

[3] Bera, A. Kumar, T. Ojha, K. Mandal, A. Screening of microemulsion properties for application in enhanced oil recovery. Fuel. **2014**, 121, 198-207.

[4] Nourafkan, E. Hu, Z. Wen, D. Controlled delivery and release of surfactant for enhanced oil recovery by nanodroplets, Fuel. **2018**, 218, 396-405

[5] Bragg, J.R., Gale, W.W., McElhannon, W.A., Davenport, O.W., Petrichuk, M.D., Ashcraft, T.L. Loudon Surfactant Flood Pilot Test. SPE/DOE 10862. Symposium on Enhanced Oil Recovery of the Society of Petroleum Engineers, Tulsa, 1982.

[6] Manning, R.K. Pope, G.A. Lake, L.W. Paul, G.W. A technical survey of polymer flooding projects. Report No. DOE/BC10327-19, US DOE, Washington, 1983.

[7] Binks, B.P. Rocher, A. Effects of temperature on water-in-oil emulsions stabilised solely by wax microparticles. J. Colloid Interface Sci. **2009**, 335, 94-104.

[8] Barnes, J.R. Smit, J.P. Shpakoff, P.G. Raney, K.H. Puerto, M.C. Phase behaviour methods for the evaluation of surfactants for chemical flooding at higher temperature reservoir conditions. SPE Improved Oil Recovery Symposium, Oklahoma, USA, 2008.

[8] Sharma, T. Kumar. G.S. Chon. B.H. Sangwaia, J.S. Thermal stability of oil-in-water Pickering emulsion in the presence of nanoparticle, surfactant, and polymer. JIEC. **2015**, 22, 324-334.

[9] Saigal, T. Dong, H. Matyjaszewski, K. Tilton, R.D. Pickering emulsions stabilized by nanoparticles with thermally responsive grafted polymer brushes. Langmuir. **2010**, 26, 15200-15209.

[10] Maurya, N.K. Mandal, A. Investigation of synergistic effect of nanoparticle and surfactant in macro emulsion based EOR application in oil reservoirs, Chem. Eng. Res. Des. **2018**, 132, 370-384.

[11] Zhang, T. Roberts, M. Bryant, S.L. Huh, H. foams and emulsions stabilized with nanoparticles for potential conformance control applications, SPE International Symposium on Oilfield Chemistry. Texas, 2009.

[12] Hu, Z. Nourafkan, E. Gao, H. Wen, D. Microemulsions stabilized by in-situ synthesized nanoparticles for enhanced oil recovery. Fuel, **2017,** 210, 272-281.

[13] Zhang, T. Espinosa, D. Yoon, K.Y. Rahmani, AR. Yu, H. Galdelas, F.M. Ryoo, S. Roberts, M. Prodanovic, M. Johnston, K.P. Milner, T.E, Bryant, S.L. Huh, C. Engineered nanoparticles as harsh-condition emulsion and foam stabilizers and as novel sensors, Offshore Technology Conference: Houston, Texas, USA, 2011.

[14] Sharma, T. Kumar, G.S. Sangwai, J.S. Enhanced oil recovery using oil-in-water (o/w) emulsion stabilized by nanoparticle, surfactant and polymer in the presence of NaCl. Geosystem Eng. **2014**, 17,195-205.

[15] Zargartalebi, M. Kharrat, R. Barati, N. Enhancement of surfactant flooding performance by the use of silica nanoparticles. Fuel. **2015**, 143, 21-27.

[16] Avila, N.L.D. De Araujo, L.L.G.C. Drexler, S. Rodrigues, J.A. Nascimento, R.S.V. Polystyrene nanoparticles as surfactant carriers for enhanced oil recovery. J. Appl. Polym. Sci. **2016**, 133, 1-7.

[17] Nourafkan, E. Hu, Z. Wen, D. Nanoparticle-enabled delivery of surfactants in porous media. J. Colloid Int. Sci. **2018**, 519, 44-57.

(18) Barnes, J.R.; Smit, J.P.; Shpakoff, P.G.; Raney, K.H.; Puerto, M.C. Phase behaviour methods for the evaluation of surfactants for chemical flooding at higher temperature reservoir conditions. SPE Improved Oil Recovery Symposium, Oklahoma, USA, 2008.

(19) Muherei, M.A.; Junin, R. Mixing Effect of anionic and nonionic surfactants on micellization. Mod. Appl. Sci. 2008, 2, 3-12.

(20) Okoli, C.; Sanchez-Dominguez, M.; Boutonnet, M.; Jaras, S.; Civera, C.; Solans, C.; Kuttuva, G.R. Comparison and functionalization study of microemulsion-prepared magnetic iron oxide nanoparticles. Langmuir. 2012, 28, 8479-8485.

[21] Mumtaz, M. Tan, I.M. Mushtaq, M. synergistic effects of surfactants mixture for foam stability measurements for enhanced oil recovery applications. Annual Technical Symposium, Al-Khobar, Saudi Arabia, 2015.

[22] Fanun, M. Properties of microemulsions with mixed non-ionic surfactants and citrus oil. Colloids. Surf. A. **2010**, 369, 246-252.

[23] Bera, A. Ojha, K. Mandal, A. Synergistic Effect of Mixed Surfactant Systems on Foam Behavior and Surface Tension. J. Surfactants Deterg. **2013**, 16, 621-630.

[24] Maghzi, A. Kharrat, R. Mohebbi, A. Ghazanfari, M.H. The impact of silica nanoparticles on the performance of polymer solution in presence of salts in polymer flooding for heavy oil recovery. Fuel. **2014**, 123, 123-132.

[25] Liftona, V.A. Microfluidics: an enabling screening technology for enhanced oil recovery (EOR). Lab Chip. **2016**, 16, 1777-1796.

[26] Elyaderani Ghalamizade, S.M. Jafari, A. Microfluidics experimental study in porous media applied for nanosilica/alkaline flooding. J. Pet. Sci. Eng. **2019**, 173, 1289-1303.

[27] Asachi, M. Hassanpour, A. Ghadiri, M. Bayly, A. Assessment of near-infrared (NIR) spectroscopy for segregation measurement of low content level ingredients. Powder Technol. **2017**, 320, 143-154.

[28] Nourafkan, E. Asachi, M. Gao, H. Raza, G. Wen, D. Synthesis of stable iron oxide nanoparticle dispersions in high ionic media. JIEC. **2017**, 50, 57-71.

[29] Wan, L.S.C. Poon, P.K.C. Effect of salts on the surface /interfacial tension and critical micelle concentration of surfactants. J. Pharm. Sci. **1969**, 58, 1562-1567.

[30] Behera, M.R. Varade, S.R. Ghosh, P. Foaming in micellar solutions: Effects of surfactant, salt, and oil concentrations. Ind. Eng. Chem. Res. **2014**, 53, 18497-18507.

[31] Yu, D. Huang, X. Deng, M. Lin, Y. Jiang, L. Huang, J. Wang, Y. Effects of inorganic and organic salts on aggregation behavior of cationic gemini surfactants, J. Phys. Chem. B. **2010**, 114, 14955-14964.

[32] Somasundaran, P. Encyclopedia of Surface and Colloid Science. Second edition, CRC Press Book, 2002.

[33] Vatanparast, H. Shahabi, F. Bahramian, A. Javadi, A. Miller, R. The role of electrostatic repulsion on increasing surface activity of anionic surfactants in the presence of hydrophilic silica nanoparticles, Sci. Rep. **2018**, 8, 1-11.

[34] Saien, J. Bahrami, M. Understanding the effect of different size silica nanoparticles and SDS surfactant mixtures on interfacial tension of n-hexane-water, J. Mol. Liq. **2016**, 224, 158-164.

[35] Biswal, N.R. Singh, J. K. Interfacial behavior of nonionic Tween 20 surfactant at oil-water interfaces in the presence of different types of nanoparticles, RSC Adv. **2016**, 6, 113307-113314.

[36] Whitby, C.P. Fornasiero, D. Ralston, J. Liggieri, L. Ravera, F. Properties of fatty amine-silica nanoparticle interfacial layers at the hexane−water interface, J. Phys. Chem. C. **2012**, 116, 3050-3058.

[37] Bernal, J.D. Fowler, R.H. A theory of water and ionic solution, with particular reference to hydrogen and hydroxyl ions. J. Chem. Phys. **1933**, 1, 515-548.

[38] Kwak, H. T. Zhang, G. Chen, S. Atlas, B. The effects of salt type and salinity on formation water viscosity and NMR responses. International Symposium of the Society of Core Analysts, Canada, 2005.

[39] Aswal, V.K.; Goyal, P.S. Dependence of the size of micelles on the salt effect in ionic micellar solutions. Chem. Phys. Lett. **2002**, 364, 44-50.

[40] Cheng, L. Mewes, D. Luke, A. Boiling phenomena with surfactants and polymeric additives: A state-of-the-art review, Int. J. Heat Mass Tran. **2007**, 50, 2744-2771.

[41] Chhabra, R.P. Richardson, J.F. Non-Newtonian flow in the process industries: Fundamentals and engineering applications, Butterworth-Heinemann, Oxford, 1999.

[42] Kovalchuk, N.M. Nowak, E. Simmons, M.J.H. Kinetics of liquid bridges and formation of satellite droplets: Difference between micellar and bi-layer forming solutions, Colloids Surf. A Physicochem. Eng. Asp. **2017**, 521, 193-203.

[43] Fogang, L.T. Sultan, A.S. Kamal, M.S. Understanding viscosity reduction of a long-tail sulfobetaine viscoelastic surfactant by organic compounds, RSC Adv. **2018**, 8, 4455-4463.

[44] Pal, N. Samanta, K. Mandal, A. A novel family of non-ionic gemini surfactants derived from sunflower oil: Synthesis, characterization and physicochemical evaluation, J. Mol. Liq. **2019**, 275 638-653.

[45] Kumar N., Mandal, A. Surfactant stabilized oil-in-water nanoemulsion: stability, interfacial tension, and rheology study for enhanced oil recovery application, Energy Fuels. **2018**, 32, 6452-6466.

[46] Tagavifar, M. Herath, S. Weerasooriya, U.P. Sepehrnoori, K. Pope, G. Measurement of microemulsion viscosity and its implications for chemical enhanced oil recovery. SPE J. **2017**, SPE-179672-PA, 1-25.

[47] Pal, N. Kumar, S. Bera, A. Mandal, A. Phase behaviour and characterization of microemulsion stabilized by a novel synthesized surfactant: Implications for enhanced oil recovery, Fuel. **2019**, 235, 995-1009.

[48] Kumar, N. Mandal, A. Thermodynamic and physicochemical properties evaluation for formation and characterization of oil-in-water nanoemulsion, J. Mol. Liq. **2018**, 266,147-159.

[49] Bai, J. Goodridge, R.D. Hague, R.J.M. Song, M. Okamoto, M. Influence of carbon nanotubes on the rheology and dynamic mechanical properties of polyamide-12 for laser sintering, Polym. Test. **2014**, 36, 95-100.

[50] Barnes, J.R. Smit, J. Smit, J. Shpakoff, G. Raney, K.H. Puerto, M. Development of surfactants for chemical flooding at difficult reservoir conditions. SPE Symposium on Improved Oil Recovery, Oklahoma, USA, 2008.

[51] Barnes, J.R. Dirkzwager, H. Smit, J. Smit, J. Navarrete, R.C. Ellison, B. Buijse, M.A. Application of internal olefin sulfonates and other surfactants to EOR. Part 1: Structure - performance relationships for selection at different reservoir conditions. SPE Improved Oil Recovery Symposium, Oklahoma, USA, 2010.

[52] Liyanage, P.J. Solairaj, S. Arachchilage, G.W.P. Linnemeyer, H.C. Kim, D.H. Weerasooriya, U. Pope, G.A. Alkaline surfactant polymer flooding using a novel class of large hydrophobe surfactants. SPE Improved Oil Recovery Symposium, Oklahoma, USA, 2012.

[53] Ali, J.A. Kolo, K. Khaksar Manshad, A. Mohammadi, A.H. Review: Recent advances in application of nanotechnology in chemical enhanced oil recovery: Effects of nanoparticles on wettability alteration, interfacial tension reduction, and flooding, Egy. J. Pet. **2018**, 27, 1371-1383.

Graphical abstract: